



Title	PREPUBLICATION: Melcherite, trigonal Ba ₂ Na ₂ Mg[Nb ₆ O ₁₉].6H ₂ O, the second natural hexaniobate, from Cajati, São Paulo, Brazil: Description and crystal structure
Authors	Andrade, MB; Atencio, D; Menezes Filho, LAD; Spratt, J
Description	© Mineralogical Society of Great Britain and Ireland 2018. This document is the author's final accepted version of the journal article. You are advised to consult the published version if you wish to cite from it.
Date Submitted	2018-05-22

1
2
3
4
5
6
7
8
9
10
11
12
13
14
15
16
17
18
19
20
21
22
23

**Melcherite, trigonal $\text{Ba}_2\text{Na}_2\text{Mg}[\text{Nb}_6\text{O}_{19}]\cdot 6\text{H}_2\text{O}$, the
second natural hexaniobate, from Cajati, São Paulo,
Brazil: Description and crystal structure**

MARCELO B. ANDRADE^{1,*}, DANIEL ATENCIO², LUIZ A.D.
MENEZES FILHO^{3,†} AND JOHN SPRATT⁴

¹Department of Physics and Interdisciplinary Science, São Carlos Institute of Physics,
University of São Paulo, Caixa Postal 369, 13560-970 São Carlos, SP, Brazil

²Departamento de Mineralogia e Geotectônica, Instituto de Geociências, Universidade de São
Paulo, Rua do Lago 562, 05508-080 São Paulo, SP, Brazil

³Instituto de Geociências, Universidade Federal de Minas Gerais, Avenida Antonio Carlos
6627, 31270-901, MG, Brazil. Deceased July 2014

⁴Core Research Laboratories, Natural History Museum, Cromwell Road, London SW7 5BD,
United Kingdom

*E-mail: mabadean@terra.com.br



24

25

ABSTRACT

26

27

28

29

30

31

32

33

34

35

36

37

38

39

40

41

42

43

44

45

46

47

48

49

50

51

52

53

54

55

56

Melcherite, ideally $\text{Ba}_2\text{Na}_2\text{Mg}[\text{Nb}_6\text{O}_{19}]\cdot 6\text{H}_2\text{O}$, occurs as a vug mineral in the carbonatite of the Jacupiranga mine, Cajati county, São Paulo state, Brazil, associated with dolomite, calcite, magnetite, pyrrhotite, tochilinite, “pyrochlore”, and fluorapatite. This is also the type locality for zirkelite, quintinite, menezesite and pauloabibite. The mineral forms irregular, tabular crystals up to 200 μm in maximum dimension. Melcherite is transparent and displays a vitreous lustre; it is beige with a white streak. It is non-fluorescent. The mineral displays perfect cleavage on $\{001\}$. Chemical composition varies from $\text{Ba}_2\text{Na}_2\text{Mg}[\text{Nb}_6\text{O}_{19}]\cdot 6\text{H}_2\text{O}$ to $(\text{BaK})(\text{NaCa})\text{Mg}[\text{Nb}_6\text{O}_{19}]\cdot 6\text{H}_2\text{O}$. Empirical formulae for the first and the second compositions are: $(\text{Ba}_{1.75}\text{K}_{0.19})_{\Sigma 1.94}(\text{Na}_{1.80}\text{Ca}_{0.19})_{\Sigma 1.99}(\text{Mg}_{0.96}\text{Mn}_{0.02}\text{Al}_{0.02})_{\Sigma 1.00}\text{Nb}_{6.02}\text{O}_{19.00}\cdot 6\text{H}_2\text{O}$ and $(\text{Ba}_{0.99}\text{K}_{1.00})_{\Sigma 1.99}(\text{Na}_{1.02}\text{Ca}_{0.96})_{\Sigma 1.98}(\text{Mg}_{0.95}\text{Mn}_{0.05})_{\Sigma 1.00}\text{Nb}_{6.02}\text{O}_{19.00}\cdot 6\text{H}_2\text{O}$, respectively. Data for a single crystal with the second composition are: trigonal, $R\bar{3}$, $a = 9.0117(6)$ Å, $c = 23.3986(16)$ Å, $V = 1645.64(19)$ Å³, $Z = 3$. Calculated density for this formula is 3.733 g/cm³, and the calculated mean refractive index is 1.924. Melcherite is a hexaniobate that has structural layers parallel to the xy plane that stack along the c-axis with simultaneous 1/3 [1 -1 0] displacement so as to produce a *R* lattice. The melcherite structure is built by layers of $[(\text{Ba},\text{K})(\text{O},\text{H}_2\text{O})_9]$ polyhedra and the $[\text{Nb}_6\text{O}_{19}]^{8-}$ super-octahedron (Lindqvist anion) interconnected by $[(\text{Na},\text{Ca})\text{O}_6]$ polyhedra. Mg^{2+} cations are bonded to six water molecules each and are not associated with Lindqvist oxygen ions. The mineral is named in honour of Geraldo Conrado Melcher (1924-2011), a pioneer in Jacupiranga carbonatite studies. Both the description and the name were approved by the CNMNC-IMA (Nomenclature Proposal 2015-018). Melcherite is the second natural hexaniobate. The first one is peterandresenite and the third is hanesmarkite.

KEYWORDS: Melcherite, new mineral, hexaniobate, crystal structure, chemical composition, Jacupiranga mine, Cajati, Brazil.

57

58

Introduction

59

60 Melcherite is the second natural hexaniobate. The first one is peterandresenite (Friis *et*
61 *al.*, 2014) and the third is hanesmarkite (Friis *et al.*, 2016). Polyoxometalates of niobium are
62 dominated by the Lindqvist hexaniobate ion, $(\text{Nb}_6\text{O}_{19})^{8-}$, and its synthesis and stability
63 requires alkaline conditions. The crystal structure of these compounds was first described by
64 Lindqvist (1953). Hexaniobates are negatively charged clusters of six mutually edge-sharing
65 NbO_6 octahedra forming a super-octahedron (Nyman, 2011). Possible polyoxoniobate
66 applications include their use as reagents in the break-down of nerve agents and in the
67 development of filter media protection against chemical warfare agents (Kinnan *et al.*, 2014).
68 Polyoxometalates have also been investigated in coordination chemistry, leading to the
69 development of hybrid organometallic hexametallates complexes (Abramov *et al.*, 2016), and
70 the synthesis of new polyoxoniobates coordinated to copper complexes (Wang *et al.*, 2008).

71 The mineral is named in honour of Geraldo Conrado Melcher (1924-2011). He was
72 professor at the Department of Mining Engineering at the Polytechnic School, University of
73 São Paulo and was also a pioneer in Jacupiranga carbonatite studies (Melcher, 1966).

74 Both the description and name were approved by the CNMNC-IMA (Nomenclature
75 Proposal 2015-018). Type material is deposited in the Museu de Geociências, Instituto de
76 Geociências, Universidade de São Paulo, Rua do Lago, 562, 05508-080 - São Paulo, SP,
77 Brazil. Specimen number: DR982. Part of the cotype sample has been deposited at the
78 University of Arizona Mineral Museum, RRUFF Project (<http://rruff.info/R130752>).

79

80

81

Occurrence

82

83 The mineral occurs in the carbonatite of the Jacupiranga mine (24°43'47"S,
84 48°06'37"W), Cajati County, São Paulo, Brazil (Menezes Filho and Martins, 1984). For
85 general information about this carbonatite please see Menezes Filho *et al.* (2015). This is also
86 the type locality for zirkelite (Hussak and Prior, 1895), quintinite (Chao and Gault, 1997),
87 menezesite (Atencio *et al.*, 2008) and pauloabibite (Menezes Filho *et al.*, 2015). Although the
88 joint occurrence of menezesite, pauloabibite and melcherite has not been observed, these
89 minerals may be genetically related. Pauloabibite is trigonal NaNbO_3 , isostructural with
90 ilmenite (Menezes Filho *et al.*, 2015). The synthetic analog of pauloabibite was reported by

91 Kinomura *et al.* (1984) and Kumata *et al.* (1990) from a two-step synthesis method, involving
92 the preparation of $\text{Na}_8\text{Nb}_6\text{O}_{19} \cdot 13\text{H}_2\text{O}$ (a hexaniobate) followed by hydrothermal reaction with
93 NaOH in a silver-lined vessel at 250 °C. Menezesite is a heteropolyoxoniobate,
94 $(\square, \text{Ba}, \text{K})_{12}(\square, \text{Mg})_3\text{Zr}_4(\text{BaNb}_{12}\text{O}_{42}) \cdot 12\text{H}_2\text{O}$, cubic (Atencio *et al.* 2008). According to Nyman
95 *et al.* (2002), the heteropolyanions of W, Mo, and V are formed simply by acidification of
96 solutions of their oxoanions. Under similar conditions, these oxoanion precursors are not
97 available for Nb, and Nb-oxo chemistry is dominated by formation of the Lindquist ion
98 $[\text{Nb}_6\text{O}_{19}]^{8-}$ (present in melcherite). However, heteropolyniobate (present in menezesite)
99 formation is favored in hydrothermal reactions of aqueous, alkaline precursor mixtures. A
100 competing phase to the formation of polyoxoniobates in hydrothermal aqueous reactions
101 involving Nb and an alkali hydroxide is NaNbO_3 , avoided by using short reaction times (i.e.,
102 24 hours or less) (Nyman *et al.*, 2002). So melcherite could be originally formed, under acid
103 conditions, and posteriorly, under basic conditions, menezesite and pauloabibite formed.

104 Quintinite, menezesite, pauloabibite and melcherite occur in the so-called
105 “intermediate zone”, characterized by a high dolomite and slightly anomalous pyrochlore
106 content. Associated minerals are dolomite, calcite, magnetite, pyrrhotite, tochilinite,
107 “pyrochlore”, pyrite, and fluorapatite. Melcherite formed as a carbonatite vug mineral.

108

109

110

Habit and physical properties

111

112 Melcherite forms irregular, tabular crystals up to 200 μm in maximum dimension (Fig.
113 1). The mineral is transparent and displays a vitreous lustre; it is beige and the streak is white.
114 It is non-fluorescent under both short (254 nm) and long wavelength (366 nm) ultraviolet
115 radiation. The mineral displays perfect cleavage on $\{001\}$. Fracture was not determined.
116 Twinning and parting were not observed. The Mohs hardness and density were not measured
117 due to the paucity of material but the calculated density is 3.733 g/cm^3 [based on the empirical
118 formula $(\text{Ba}_{0.99}\text{K}_{1.00})_{\Sigma 1.99}(\text{Na}_{1.02}\text{Ca}_{0.96})_{\Sigma 1.98}(\text{Mg}_{0.95}\text{Mn}_{0.05})_{\Sigma 1.00}\text{Nb}_{6.02}\text{O}_{19.00} \cdot 6\text{H}_2\text{O}$]. Refractive
119 indices were not measured due to paucity of material. The mean refractive index is estimated
120 as 1.924 using the Gladstone-Dale relationship.

121

122

123

Mineral chemistry

124

125

126 Melcherite crystals were embedded in epoxy resin and polished. In the backscattered
127 electron images, we can see that the crystals are zoned (Fig. 2). The chemical analyses (Table
128 1) were done by means of a Cameca SX100 electron microprobe (WDS mode, 15 kV, 10 nA,
129 20 μm beam diameter). H_2O was inferred from the crystal structure determination of
130 melcherite. H_2O was initially assumed by difference prior to the matrix correction (PAP) and
131 then calculated by stoichiometry post matrix correction due to software limitations. Analyses
132 from the brighter areas of the melcherite crystal, (Fig. 2 backscattered electron image) have
133 the following composition:

134 $(\text{Ba}_{1.75}\text{K}_{0.19})_{\Sigma 1.94}(\text{Na}_{1.80}\text{Ca}_{0.19})_{\Sigma 1.99}(\text{Mg}_{0.96}\text{Mn}_{0.02}\text{Al}_{0.02})_{\Sigma 1.00}\text{Nb}_{6.02}\text{O}_{19.00}\cdot 6\text{H}_2\text{O}$ (mean of 4 point
135 analyses). Those from the darker areas correspond to
136 $(\text{Ba}_{0.99}\text{K}_{1.00})_{\Sigma 1.99}(\text{Na}_{1.02}\text{Ca}_{0.96})_{\Sigma 1.98}(\text{Mg}_{0.95}\text{Mn}_{0.05})_{\Sigma 1.00}\text{Nb}_{6.02}\text{O}_{19.00}\cdot 6\text{H}_2\text{O}$ (mean of 8 point
137 analyses). The enrichment in Ba is coupled to the enrichment in Na and depletion of K and
138 Ca. The analyses were obtained in points of several shades of gray observed in backscattered
139 electron images distributed in different crystals. These analyses were ordered in ascending Ba
140 apfu numbers, numbered from 1 to 25, and served as the basis for the construction of the
141 graph of Figure 3.

142 Chemical composition varies from $\text{Ba}_2\text{Na}_2\text{Mg}[\text{Nb}_6\text{O}_{19}]\cdot 6\text{H}_2\text{O}$ to
143 $(\text{BaK})(\text{NaCa})\text{Mg}[\text{Nb}_6\text{O}_{19}]\cdot 6\text{H}_2\text{O}$. Coupled heterovalent substitutions at two sites are verified.
144 As discussed by Hatert and Burke (2008), where a heterovalent substitution occurs at a given
145 crystallographic site, the charge balance can also be maintained by coupling this substitution
146 to another heterovalent substitution at a different site. At the *Ba* site, the atom Ba^{2+} is
147 progressively replaced by K^+ , and to maintain charge balance, the atom Na^+ is progressively
148 replaced by Ca^{2+} at the *Na* site. The substitution mechanism is $\text{Ba}^{2+} + \text{K}^+ \leftrightarrow \text{Na}^+ + \text{Ca}^{2+}$. The
149 boundary site-occupancies between the two members of the series is
150 $(\text{BaK})(\text{NaCa})\text{Mg}[\text{Nb}_6\text{O}_{19}]\cdot 6\text{H}_2\text{O}$. We could imagine a solid solution series from
151 $\text{Ba}_2\text{Na}_2\text{Mg}[\text{Nb}_6\text{O}_{19}]\cdot 6\text{H}_2\text{O}$ to $\text{K}_2\text{Ca}_2\text{Mg}[\text{Nb}_6\text{O}_{19}]\cdot 6\text{H}_2\text{O}$, with two mineral species, but the
152 composition varies only from the first end-member to the intermediate member. As no
153 analyses correspond to predominant K and Ca, only one mineral species is defined.

154 The formula $\text{BaCa}_2\text{Mg}[\text{Nb}_6\text{O}_{19}]\cdot 6\text{H}_2\text{O}$ (Andrade *et al.*, 2015) is incorrect because Na
155 was not identified. The change in formula was previously approved executively by CNMNC
156 IMA Newsletter No. 29 (Hålenius *et al.*, 2016): "Soon after the approval of the new mineral

157 melcherite (IMA No. 2015-018; see CNMNC Newsletter 25), the authors of the proposal have
158 communicated results of subsequent analytical work on this mineral, which verifies essential
159 contents of sodium. The new data were examined carefully by the CNMNC officers and were
160 found reliable. The revised simplified formula, $\text{Ba}_2\text{Na}_2\text{Mg}[\text{Nb}_6\text{O}_{19}]\cdot 6\text{H}_2\text{O}$, has been approved
161 executively." A fragment of the darker part was extracted from the polished section for crystal
162 structure determination.

163

164

165

Crystal structure determination

166

167 Powder X-ray diffraction data (XRD) were obtained using a Siemens D5000
168 diffractometer equipped with a Göbel mirror and a position-sensitive detector using $\text{CuK}\alpha$
169 radiation and 40 kV and 40 mA at the Instituto de Geociências of the Universidade de São
170 Paulo (Table 2). Unit cell parameters refined from the powder data are as follows: Trigonal,
171 Space Group: $R\bar{3}$, $a = 9.022(2)$ Å, $c = 23.410(6)$ Å, $V = 1650.2(8)$ Å³, $Z = 3$.

172 A single-crystal X-ray study was carried-out using a Bruker APEX II CCD
173 diffractometer with graphite-monochromated $\text{MoK}\alpha$ ($\lambda = 0.71073$ Å) radiation and gave the
174 following data: Trigonal, Space Group: $R\bar{3}$, $a = 9.0117(6)$ Å, $c = 23.3986(16)$ Å, $c : a =$
175 2.5965 , $V = 1645.64(19)$ Å³, $Z = 3$. The X-ray absorption correction was applied to intensity
176 data using the program SADABS from Bruker.

177 The SHELXL-97 package (Sheldrick, 2008) was used for the direct methods
178 structure solution and its subsequent refinement. The Ba and Na sites were refined assuming
179 full but joint occupation by Ba/K and Na/Ca respectively, which yielded occupancy values
180 close to those indicated by the empirical formula based on the EMP analysis. A final
181 difference Fourier synthesis allowed the H atom positions of the water molecule to be located,
182 which were then refined with soft restraints of 0.86 Å on the O-H distances and 1.40 Å on the
183 H-H distance, and with U_{iso} values fixed at ~1.5 times that of the O atom. Refinement of this
184 final model converged to an R1 of 0.017 and the crystal chemical formula obtained is
185 $(\text{Ba}_{1.06}\text{K}_{0.94})(\text{Na}_{1.09}\text{Ca}_{0.91})\text{Nb}_6\text{Mg}[\text{O}_{18.98}(\text{OH})_{0.02}]_{\Sigma 19.00}$, where a small fraction of the oxygen
186 atoms in the hexaniobate polyanion is assumed to be replaced by OH groups in order to
187 balance the slight positive charge deficiency associated with the Ba/K and Na/Ca sites. $6\text{H}_2\text{O}$.
188 Details of the data collection and structure refinement are given in Tables 3 and 4. Selected

189 bond distances and associated bond -valence sum calculations, using the parameters of Brese
190 and O'Keefe (1991), are given in Table 5.

191 Melcherite is a hexaniobate that has structural layers parallel to the xy plane that
192 stack along the *c*-axis with simultaneous 1/3 [1 -1 0] displacement so as to produce a *R* lattice.
193 The melcherite structure (Figs. 4 and 5) is built by layers of [(Ba,K)(O,H₂O)₉] polyhedra and
194 the [Nb₆O₁₉]⁸⁻ super-octahedron (Lindqvist anion) interconnected by [(Na,Ca)O₆] polyhedra.
195 There is a significant distortion present in the Nb-O octahedron forming the hexaniobate
196 polyanion, as measured by the octahedral angle variance (OAV), 113.650, and quadratic
197 elongation (OQE), 1.040, indices (Robinson et al. 1971). The results are comparable to the
198 NbO₆ octahedra present in the crystal structure of peterandresenite and hanesmarkite (Table
199 6). Ba/K is coordinated by six oxygens and three water molecules. The Na/Ca is coordinated
200 by six oxygen atoms in a distorted octahedron and the OAV and OQE values are 354.100 and
201 1.113, respectively. Mg²⁺ cations are bonded to six water molecules each and are not
202 associated with Lindqvist oxygen ions. The comparison with MnO₆ in peterandresenite and
203 hanesmarkite shows that the octahedral coordination of the Mg cation is relatively
204 undistorted, as indicated by the indice values of OAV, 12.285, and OQE, 1.003 (Table 6).

205 The mineral is structurally similar to the synthetic compounds
206 Cs₆Na₂(Nb₆O₁₉).18H₂O and Rb₆(H₂Nb₆O₁₉).19H₂O, studied by Nyman *et al.* (2006) (Table 7).
207 They have the same space group of melcherite, *R*-3. The unit cell dimensions and
208 arrangement of Lindqvist ion [Nb₆O₁₉]⁸⁻ are very similar. The crystallographic parameters of
209 melcherite are compared with those of the other hexaniobate minerals in Table 8.

210

211

212

Acknowledgements

213 We acknowledge the Sao Paulo Research Foundation for financial support (Grants:
214 2011/22407-0 and 2013/03487-8); the Principal Editor, Peter Williams, the reviewer Peter
215 Leverett and anonymous reviewers, and the members of the Commission on New Minerals
216 and Mineral Names of the International Mineralogical Association (CNMNC-IMA) for their
217 helpful suggestions and comments.

218

219

220

221

References

222

223 Andrade, M.B., Atencio, D. and Menezes Filho, L.A.D. (2015) Melcherite, IMA 2015-018.

224 CNMNC Newsletter No. 25, June 2015, page 547; *Mineralogical Magazine*, **79**, 541-
225 547.

226 Abramov, P.A., Vicent, C., Kompankov, N.B., Gushchin, A.L. and Sokolov, M.N. (2016)
227 Coordination of $\{C_5Me_5Ir\}^{2+}$ to $[M_6O_{19}]^{8-}$ (M = Nb, Ta) – Analogies and Differences
228 between Rh and Ir, Nb and Ta. *European Journal of Inorganic Chemistry*, **1**, 154-160.

229 Atencio, D., Coutinho, J.M.V., Doriguetto, A.C., Mascarenhas, Y.P., Ellena, J.A. and Ferrari,
230 V.C. (2008) Menezesite, the first natural heteropolyniobate, from Cajati, São Paulo,
231 Brazil: Description and crystal structure. *American Mineralogist*, **93**, 81-87.

232 Brese, N.E. and O'keeffe, M. (1991) Bond-valence parameters for solids. *Acta*
233 *Crystallographica Section B: Structural Science*, **47(2)**, 192-197.

234 Chao, G.Y. and Gault, R.A. (1997) Quintinite-2*H*, quintinite-3*T*, charmarite-2*H*, charmarite-
235 3*T* and caresite-3*T*, a new group of carbonate minerals related to the hydrotalcite-
236 manasseite group. *Canadian Mineralogist*, **35**, 1541-1549.

237 Friis, H., Larsen, A.O., Kampf, A.R., Evans, R.J., Selbekk, R.S., Sánchez, A.A. and Kihle, J.
238 (2014) Peterandresenite, $Mn_4Nb_6O_{19} \cdot 14H_2O$, a new mineral containing the Lindqvist
239 ion from a syenite pegmatite of the Larvik Plutonic Complex, southern Norway.
240 *European Journal of Mineralogy*, **26**, 567-576.

241 Friis, H., Weller, M.T. and Kampf, A.R. (2016) Hansesmarkite, $Ca_2Mn_2Nb_6O_{19} \cdot 20H_2O$, a
242 new hexaniobate from a syenite pegmatite in the Larvik Plutonic Complex, southern
243 Norway. *Mineralogical Magazine* (in press).
244 DOI: <https://doi.org/10.1180/minmag.2016.080.109>

245 Hålenius, U., Hatert, F., Pasero, M. and Mills, S.J. (2016) New minerals and nomenclature
246 modifications approved in 2015 and 2016. CNMNC Newsletter 29. *Mineralogical*
247 *Magazine*, **80**, 199-205,

248 Hatert, F. and Burke, E.A.J. (2008) The IMA-CNMNC dominant-constituent rule revisited
249 and extended. *Canadian Mineralogist*, **46**, 717-728.

250 Hussak, E. and Prior, G.T. (1895) Lewisite and zirkelite, two new Brazilian minerals.
251 *Mineralogical Magazine*, **11**, 80-88.

252 Kinnan, M.K., Creasy, W.R., Fullmer, L.B., Schreuder-Gibson, H.L. and Nyman, M. (2014)
253 Nerve Agent Degradation with Polyoxoniobates. *European Journal of Inorganic*

254 *Chemistry*, **2014(14)**, 2361-2367.

255 Kinomura, N., Kumata, N., and Muto, F. (1984) A new allotropic form with ilmenite-type
256 structure of NaNbO_3 . *Materials Research Bulletin*, **19**, 299–304.

257 Kumata, N., Kinomura, N., and Muto, F. (1990) Crystal structure of ilmenite-type LiNbO_3
258 and NaNbO_3 . *Journal of the Ceramic Society of Japan*, **98**, 384–388.

259 Lindqvist, I. (1953) The structure of the hexaniobate ion in $7\text{Na}_2\text{O}\cdot 6\text{Nb}_2\text{O}_5\cdot 32\text{H}_2\text{O}$. *Arkiv for*
260 *Kemi*, **5(3)**, 247-250.

261 Melcher, G.C. (1966) The carbonatites of Jacupiranga, São Paulo, Brazil. Pp. 169-181 in:
262 *Carbonatites* (O.F. Tuttle and J. Gittins, editors). John Wiley and Sons, New York.

263 Menezes Filho, L.A.D., Atencio, D., Andrade, M.B., Downs, R.T., Chaves, M.L.S.C.,
264 Romano, A.W., Scholz, R. and Persiano, A.I.C. (2015) Pauloabibite, trigonal NaNbO_3 ,
265 isostructural with ilmenite, from the Jacupiranga carbonatite, Cajati, São Paulo, Brazil.
266 *American Mineralogist*, **100**, 442-446.

267 Menezes Filho, L.A.D. and Martins, J.M. (1984) The Jacupiranga mine, São Paulo, Brazil.
268 *Mineralogical Record*, **15**, 261-270.

269 Nyman, M. (2011) Polyoxoniobate chemistry in the 21st century. *Dalton Transactions*,
270 **40(32)**, 8049-8058.

271 Nyman, M., Alam, T.M., Bonhomme, F., Rodriguez, M.A., Frazer, C.S. and Welk, M.E.
272 (2006) Solid-State structures and solution behaviour of alkali salts of the $[\text{Nb}_6\text{O}_{19}]^{8-}$
273 Lindqvist Ion. *Journal of Cluster Science*, **17**, 197-219.

274 Nyman, M., Bonhomme, F., Alam, T.M., Rodriguez, M.A., Cherry, B.R., Krumhansl, J.L.,
275 Nenoff, T.M., and Sattler, A.M. (2002) A general synthetic procedure for
276 heteropolyniobates. *Science*, **297**, 996–998.

277 Wang J.P., Niu, H.Y. and Niu, J.Y. (2008) A novel Lindqvist type polyoxoniobate
278 coordinated to four copper complex moieties: $\{\text{Nb}_6\text{O}_{19}[\text{Cu}(2,2'\text{-bipy})]_2[\text{Cu}(2,2'\text{-}$
279 $\text{bipy})_2]_2\}\cdot 19\text{H}_2\text{O}$. *Inorganic Chemistry Communications*, **11(1)**, 63-65.

280

281

282 TABLE 1. Chemical composition of melcherite from the Cajati mine (in wt%).

283 TABLE 2. X-ray powder diffraction data for melcherite.

284 TABLE 3. Structure refinement results for melcherite.

285 TABLE 4. Final fractional coordinates and displacement parameters of atoms in melcherite.

286 TABLE 5. Selected bond lengths and bond valences of the refined melcherite structure.

287 TABLE 6. Selected interatomic bond lengths (Å) and octahedral distortion indices for
288 melcherite ($\text{Ba}_2\text{Na}_2\text{MgNb}_6\text{O}_{19}\cdot 6\text{H}_2\text{O}$), peterandresenite ($\text{Mn}_4\text{Nb}_6\text{O}_{19}\cdot 14\text{H}_2\text{O}$) and
289 hanesmarkite ($\text{Ca}_2\text{Mn}_2\text{Nb}_6\text{O}_{19}\cdot 20\text{H}_2\text{O}$).

290 TABLE 7. Comparative data for melcherite and synthetic compounds (all trigonal, *R*-3).

291 TABLE 8. Comparison of melcherite with other naturally-occurring hexaniobates.

292

293

294

295

296

297

298

299

300

301

302

303

304

305

306

307

308

309

310

311 FIG. 1. Melcherite from the Cajati mine, São Paulo, Brazil.

312 FIG. 2. Backscattered electron image of melcherite.

313 FIG. 3. Chemical variability in melcherite.

314 FIG. 4. Crystal structure of melcherite. (Ba,K) = yellow; (Na,Ca) = pink; Mg = green; Nb =

315 blue; O = red and OW = grey.

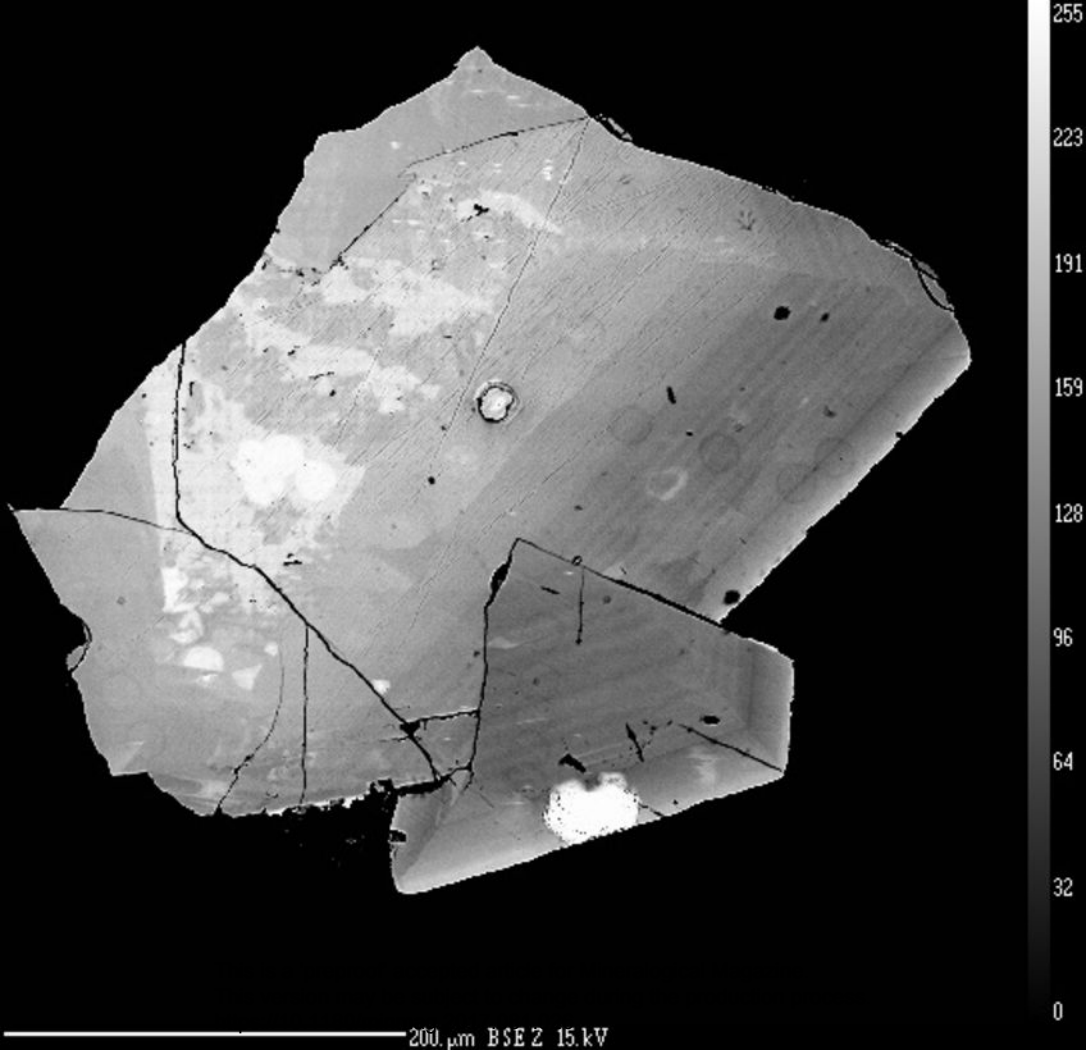
316 FIG. 5. Lindquist polyanions $[\text{Nb}_6\text{O}_{19}]^{8-}$ stacking sequence in the crystal structure of

317 melcherite.

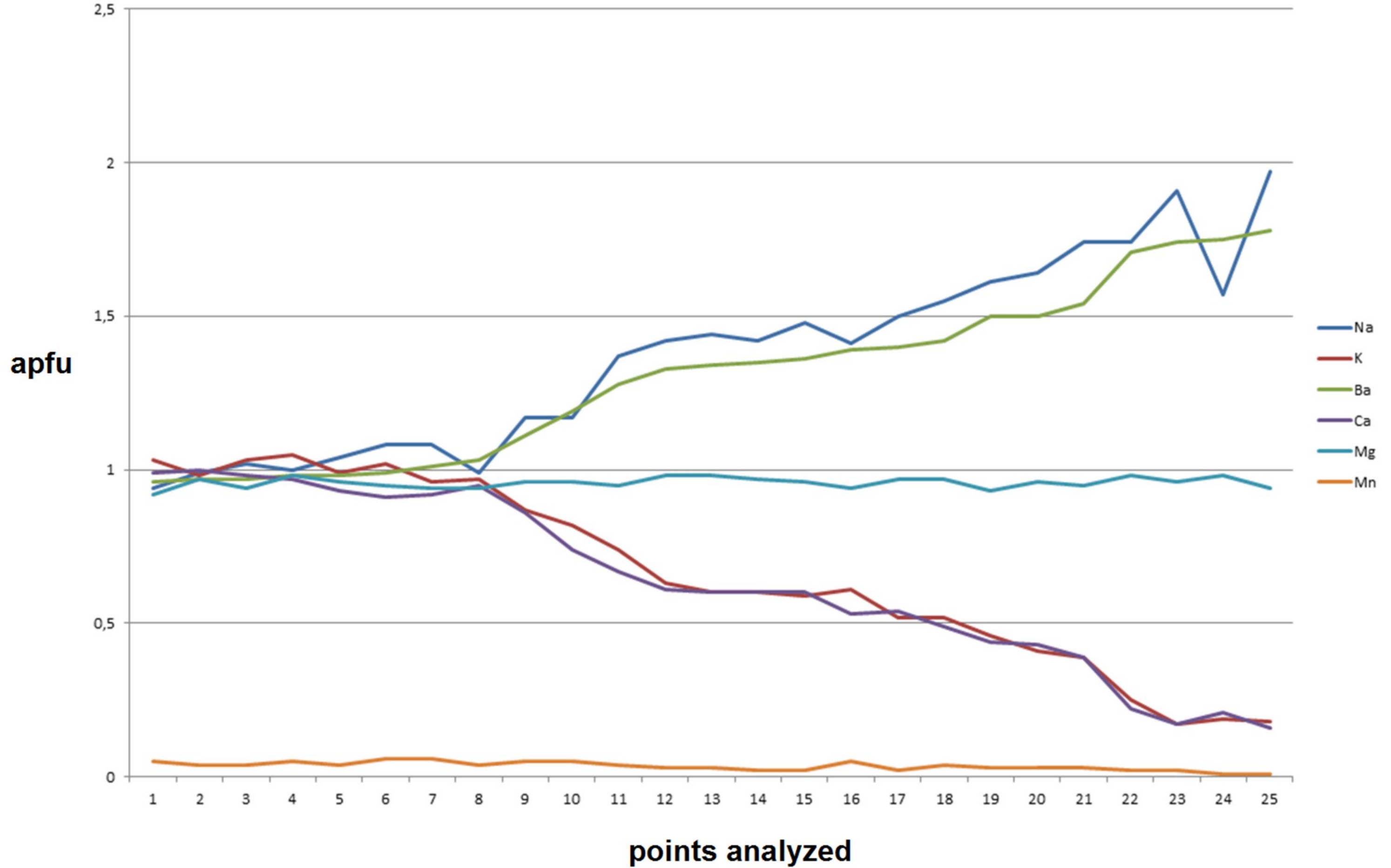
318

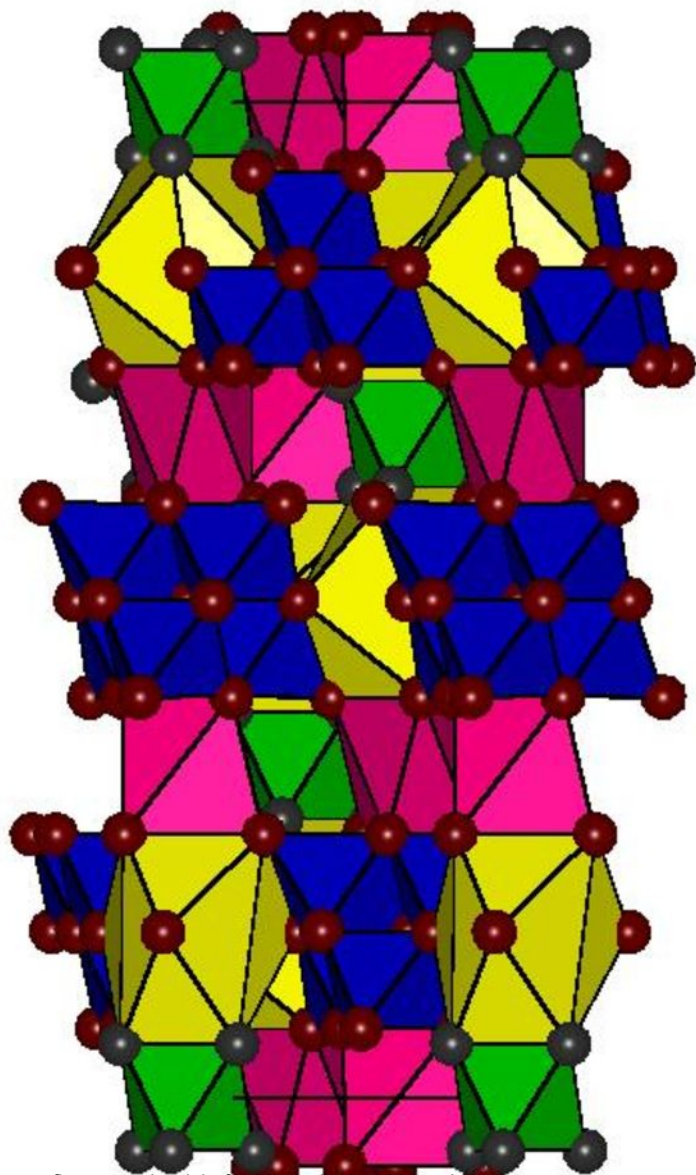
200 μm





200. μm BSE Z 15. kV





This is a 'preproof' accepted article for *Mineralogical Magazine*.
This version may be subject to change during the production process.
<https://10.1180/minmag.2017.081.026>

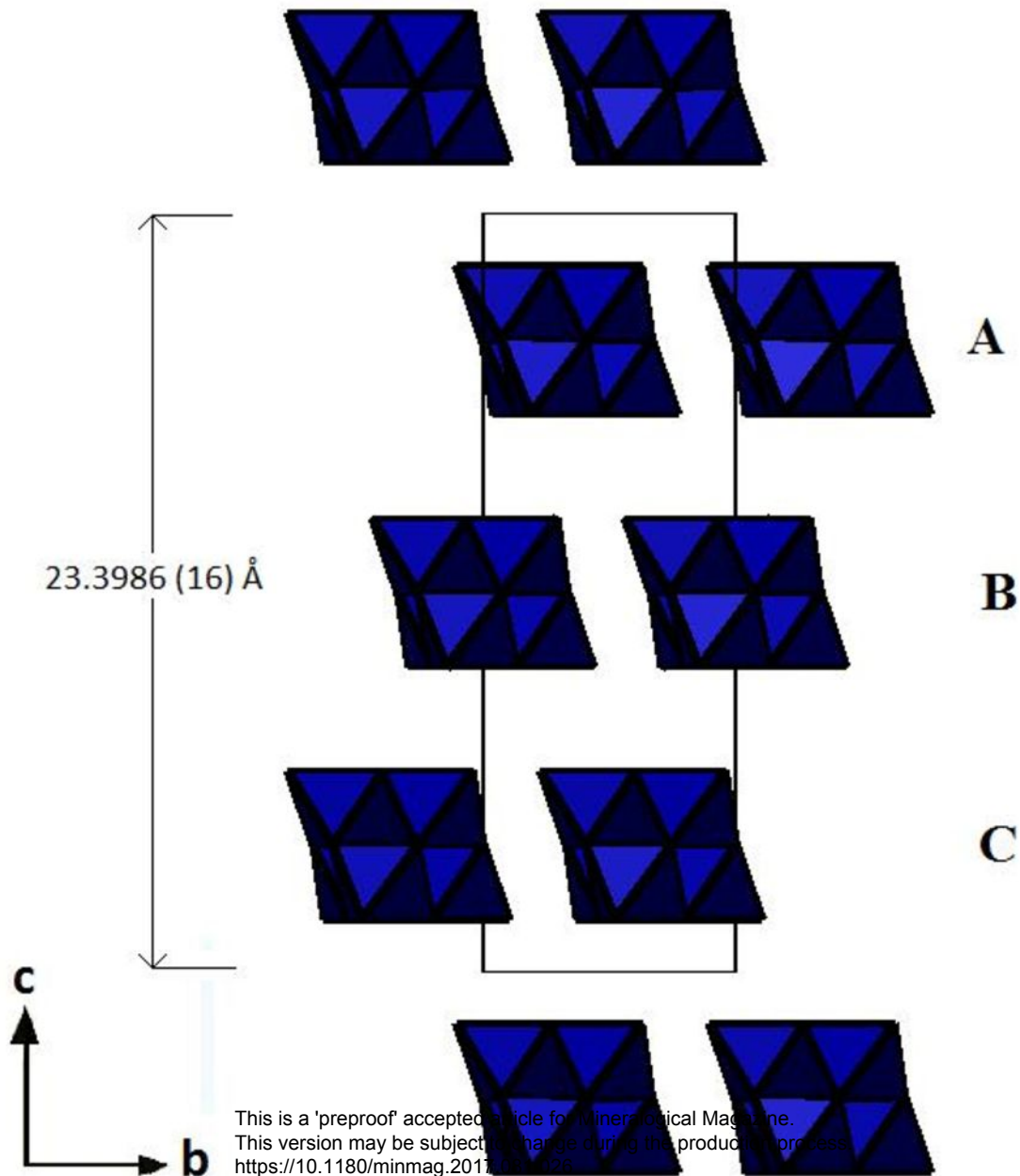


TABLE 1. Chemical composition of melcherite from the Cajati mine (in wt%).

Constituent	1	Range	Standard deviation	2	Range	Standard deviation	Probe standard
K ₂ O	0.70	0.61-0.89	0.13	3.88	3.71-4.07	0.14	orthoclase jadeite
Na ₂ O	4.30	3.76-4.68	0.42	2.60	2.41-2.76	0.13	barite
BaO	20.66	20.29-20.92	0.27	12.44	12.13-12.91	0.29	wollastonite
CaO	0.83	0.70-0.97	0.14	4.41	4.20-4.60	0.16	forsterite
MgO	3.00	2.90-3.06	0.08	3.15	3.07-3.23	0.06	pyrophanite
MnO	0.09	0.06-0.13	0.03	0.28	0.22-0.38	0.06	corundum
Al ₂ O ₃	0.08	0.07-0.10	0.02	0.02	b.d.-0.08	0.03	
Nb ₂ O ₅	61.74	61.21-62.21	0.43	65.79	65.22-66.27	0.37	Nb
SiO ₂	0.02	b.d.l.-0.06	0.03	0.00	b.d.l.-b.d.l.	0.00	wollastonite
H ₂ O	8.35			8.90			
Total	99.77			101.47			

Note: b.d.l. = below detection limits.

1. (Ba_{1.75}K_{0.19})_{Σ1.94}(Na_{1.80}Ca_{0.19})_{Σ1.99}(Mg_{0.96}Mn_{0.02}Al_{0.02})_{Σ1.00}Nb_{6.02}O_{19.00}·6H₂O (n = 4)
2. (Ba_{0.99}K_{1.00})_{Σ1.99}(Na_{1.02}Ca_{0.96})_{Σ1.98}(Mg_{0.95}Mn_{0.05})_{Σ1.00}Nb_{6.02}O_{19.00}·6H₂O (n = 8)

TABLE 2. X-ray powder diffraction data for melcherite.

$d_{obs.}(\text{\AA})$	$d_{calc.}(\text{\AA})$	$I_{obs.}$	h	k	l
11.337	11.705	6	0	0	2
7.805	7.813	100	0	1	0
	7.803		0	0	3
7.410	7.411	14	0	1	1
6.505	6.499	7	0	1	2
5.906	5.853	6	0	0	4
4.508	4.511	10	1	1	0
4.018	4.016	8	0	1	5
3.904	3.907	22	0	2	0
	3.905		1	1	3
3.852	3.853	21	0	2	1
3.250	3.249	33	0	2	4
	3.249		1	1	5
3.074	3.074	9	0	1	7
2.952	2.953	13	1	2	0
	2.951		1	1	6
2.861	2.863	8	1	2	2
2.740	2.740	8	0	1	8
2.637	2.637	8	1	2	4
2.243	2.245	6	2	2	1
	2.243		0	1	10
2.165	2.166	30	0	3	6
	2.165		0	2	9
2.160	2.158	12	1	3	1
2.078	2.079	4	1	2	8
	2.078		1	1	10

2.053	2.055	5	0	3	7
	2.053		0	1	11
2.034	2.032	4	1	3	4
	2.032		2	2	5
1.836	1.835	4	1	2	10
1.703	1.704	5	2	2	9
1.629	1.629	4	2	3	6
1.562	1.562	5	1	4	6
	1.562		0	4	9

TABLE 3. Structure refinement results for melcherite.

Ideal chemical formula	Ba ₂ Na ₂ Mg[Nb ₆ O ₁₉].6H ₂ O
crystal size (mm)	0.07 × 0.05 × 0.05 mm
Space group	<i>R</i> -3
<i>a</i> (Å)	9.0117(6)
<i>c</i> (Å)	23.3986(16)
<i>V</i> (Å ³)	1645.64(19)
<i>Z</i>	3
ρ_{cal} (g/cm ³)	3.748
λ (Å)	0.71073
μ (mm ⁻¹)	5.46
2 θ max. for data collection(°)	≤66.38
No. of reflections collected	5316
No. of independent reflections	1403
No. of reflections with $I > 2\sigma(I)$	1319
No. of parameters refined	65
R_{int}	0.022
Final <i>R</i> factors [$I > 2\sigma(I)$]	$R_1 = 0.017$, $wR_2 = 0.042$
Final <i>R</i> factors (all data)	$R_1 = 0.019$, $wR_2 = 0.041$
Goodness-of-fit	1.13
Largest diff. peak and hole	1.30 and -1.59 e.Å ⁻³
weighting scheme: $w = 1/[\sigma^2(F_o^2) + (0.0146P)^2 + 5.6144P]$, where $P = [\max(0, F_o)^2 + (2F_c)^2]/3$.	

TABLE 4. Final fractional coordinates and displacement parameters of atoms in melcherite.

Atom	x	y	z	Occ.	U_{eq}	U_{11}	U_{22}	U_{33}	U_{23}	U_{13}	U_{12}
Ba	0.6667	0.3333	0.172426 (14)	0.5325 (19)	0.01366 (10)	0.01099 (12)	0.01099 (12)	0.01899 (16)	0.000	0.000	0.00550 (6)
K	0.6667	0.3333	0.172426 (14)	0.4674 (19)	0.01366 (10)	0.01099 (12)	0.01099 (12)	0.01899 (16)	0.000	0.000	0.00550 (6)
Nb	0.50011 (2)	0.58932 (2)	0.109104 (6)		0.00677 (6)	0.00634 (8)	0.00681 (9)	0.00773 (8)	-0.00028 (5)	0.00039 (5)	0.00372 (6)
Ca	0.6667	0.3333	0.01125 (4)	0.457 (10)	0.0101 (3)	0.0114 (4)	0.0114 (4)	0.0074 (5)	0.000	0.000	0.0057 (2)
Na	0.6667	0.3333	0.01125 (4)	0.543 (10)	0.0101 (3)	0.0114 (4)	0.0114 (4)	0.0074 (5)	0.000	0.000	0.0057 (2)
Mg	0.6667	0.3333	0.3333		0.0111 (3)	0.0093 (5)	0.0093 (5)	0.0148 (7)	0.000	0.000	0.0046 (2)
O1	0.52940 (18)	0.80056 (17)	0.06922 (6)		0.0092 (2)	0.0085 (6)	0.0081 (6)	0.0110 (6)	0.0017 (4)	0.0016 (4)	0.0042 (5)
O2	0.62705 (19)	0.52389 (19)	0.06912 (6)		0.0140 (3)	0.0114 (6)	0.0130 (7)	0.0182 (7)	-0.0022 (5)	0.0030 (5)	0.0066 (6)
O3	0.66867 (17)	0.74208 (18)	0.16615 (5)		0.0099 (2)	0.0072 (6)	0.0121 (6)	0.0103 (5)	-0.0021 (5)	-0.0006 (4)	0.0047 (5)
O4	0.3333	0.6667	0.1667		0.0081 (6)	0.0077 (9)	0.0077 (9)	0.0090 (13)	0.000	0.000	0.0039 (4)
OW5	0.2005 (2)	0.1518 (2)	0.05373 (8)		0.0184 (3)	0.0121 (7)	0.0107 (7)	0.0327 (9)	-0.0050 (6)	-0.0064 (6)	0.0060 (6)
H51	0.229 (4)	0.255 (2)	0.0579 (13)		0.030						
H52	0.286 (3)	0.142 (4)	0.0566 (13)		0.030						

TABLE 5. Selected bond lengths and bond valences of the refined melcherite structure.

Bond	Bond length	BV(v.u)	Σ
(Ba,K)-O3	2.7189(14)	0.261(x2)	0.522
(Ba,K)-O3	2.7190(14)	0.261	0.261
(Ba,K)-OW5	2.9923(18)	0.125(x3)	0.375
(Ba,K)-O2	3.0875(15)	0.096(x3)	0.288
			1.446
Nb-O1	2.0154(13)	0.754	0.754
Nb-O1	2.0161(13)	0.753	0.753
Nb-O2	1.7906(14)	1.385	1.385
Nb-O3	1.9691(13)	0.855	0.855
Nb-O3	1.9731(13)	0.845	0.845
Nb-O4	2.3678(2)	0.291	0.291
			4.883
(Na,Ca)-O2	2.3501(15)	0.286(x3)	0.858
(Na,Ca)-O1	2.4476(15)	0.2203(x3)	0.660
			1.518
Mg-OW5	2.0602(16)	0.371	0.371
Mg-OW5	2.0603(16)	0.371(x5)	1.484
			2.226
O1-Nb	2.0154(16)	0.754	0.754
O1-Nb	2.0161(16)	0.753	0.753
O1-(Na,Ca)	2.4476(15)	0.220	0.220
			1.727
O2-Nb	1.7906(14)	1.385	1.385
O2-(Na,Ca)	2.3501(15)	0.286	0.286
O2-(Ba,K)	3.0875(15)	0.080	0.096
			1.767
O3-Nb	1.9691 (13)	0.855	0.855
O3-Nb	1.9731 (13)	0.845	0.845
O3-(Ba,K)	2.7189 (14)	0.261	0.261
			1.961
O4-Nb	2.3678 (2)	0.291(x6)	1.746
OW5-Mg	2.0603 (16)	0.371	0.371
OW5-(Ba,K)	2.9923 (18)	0.125	0.125
			0.496

TABLE 6. Selected interatomic bond lengths (Å) and octahedral distortion indices for melcherite ($\text{Ba}_2\text{Na}_2\text{MgNb}_6\text{O}_{19}\cdot 6\text{H}_2\text{O}$), peterandresenite ($\text{Mn}_4\text{Nb}_6\text{O}_{19}\cdot 14\text{H}_2\text{O}$) and hansesmarkite ($\text{Ca}_2\text{Mn}_2\text{Nb}_6\text{O}_{19}\cdot 20\text{H}_2\text{O}$).

	melcherite		peterandresenite ¹		hansesmarkite ²	
Nb-O1	2.0154(13)	Nb1-O1	2.3982(1)	Nb1-O1	2.3990(6)	
Nb-O1	2.0161(13)	Nb1-O2	1.7685(8)	Nb1-O2	1.780(1)	
Nb-O2	1.7906(14)	Nb1-O3	1.9767(8)	Nb1-O3	1.962(1)	
Nb-O3	1.9691(13)	Nb1-O4	1.9799(6)	Nb1-O4	1.973(1)	
Nb-O3	1.9731(13)	Nb1-O5	2.0080(6)	Nb1-O5	2.020(1)	
Nb-O4	2.3678(2)	Nb1-O6	2.0290(8)	Nb1-O6	2.034(1)	
Mean	2.022	Mean	2.027	Mean	2.028	
OV*	10.513	OV	10.506	OV	10.723	
OAV	113.650	OAV	132.281	OAV	119.622	
OQE	1.040	OQE	1.046	OQE	1.042	
Mg-OW5	2.0602(16)	Nb2-O1	2.3679(1)	Nb2-O1	2.3576(6)	
Mg-OW5	2.0603(16)	Nb2-O3	1.9716(8)	Nb2-O4	1.977(1)	
Mean	2.060	Nb2-O3	1.9716(8)	Nb2-O5	2.029(1)	
		Nb2-O6	2.0208(8)	Nb2-O7	1.766(1)	
OV	11.603	Nb2-O6	2.0208(8)	Nb2-O8	1.982(1)	
OAV	12.285	Nb2-O7	1.777(1)	Nb2-O9	2.019(1)	
OQE	1.003	Mean	2.021	Mean	2.021	
(Na,Ca)-O2	2.3501(15)	OV	10.522	OV	10.714	
(Na,Ca)-O1	2.4476(15)	OAV	110.055	OAV	108.276	
		OQE	1.039	OQE	1.039	
OV	15.689					
OAV	354.100	Mn1-O2	2.0645	Nb3-O1	2.3764(6)	
OQE	1.113	Mn1-O2	2.0645	Nb3-O3	1.956(1)	
		Mn1-O5	2.220	Nb3-O6	2.033(1)	
		Mn1-O6	2.3250	Nb3-O8	1.979(1)	
		Mn1-O6	2.3250	Nb3-O9	2.010(1)	
		Mn1-O8	2.253(2)	Nb3-O10	1.785(1)	
		Mean	2.208	Mean	2.023	
		OV	13.518	OV	10.691	
		OAV	146.530	OAV	121.348	
		OQE	1.044	OQE	1.044	
		Mn2-O7	2.088(1)	Mn-O5	2.230(1)	
		Mn2-O9	2.106(2)	Mn-O6	2.208(1)	
		Mn2-O10	2.237(1)	Mn-O7	2.050(1)	
		Mn2-O10	2.237(1)	Mn-O9	2.254(1)	
		Mn2-O11	2.240(1)	Mn-O11	2.149(2)	
		Mn2-O11	2.240(1)	Mn-O12	2.180(2)	
		Mean	2.191	Mean	2.178	
		OV	13.992	OV	13.417	
		OAV	4.489	OAV	104.704	
		OQE	1.003	OQE	1.030	

1: Friis *et al.* (2014); 2: Friis *et al.* (2016)

*OV = octahedral volume, OAV = octahedral angle variance, and OQE = octahedral quadratic elongation (Robinson *et al.* 1971).

TABLE 7. Comparative data for melcherite and synthetic compounds (all trigonal, $R\bar{3}$).

	chemical formula	unit cell parameters (Å)	
melcherite*	$\text{Ba}_2\text{Na}_2\text{Mg}[\text{Nb}_6\text{O}_{19}]\cdot 6\text{H}_2\text{O}$	$a = 9.0117(6)$	$c = 23.3986(16)$
synthetic [†]	$\text{Cs}_6\text{Na}_2(\text{Nb}_6\text{O}_{19})\cdot 18(\text{H}_2\text{O})$	$a = 12.609(2)$	$c = 22.745(5)$
synthetic [†]	$\text{Rb}_6(\text{H}_2\text{Nb}_6\text{O}_{19})\cdot 19(\text{H}_2\text{O})$	$a = 12.271(2)$	$c = 20.686(3)$

*This work.

[†] Nyman *et al.* (2006).

TABLE 8. Comparison of melcherite with other naturally-occurring hexaniobates.

Name	melcherite	peterandresenite ¹	hansesmarkite ²
Formula	Ba ₂ Na ₂ Mg Nb ₆ O ₁₉ •6H ₂ O	Mn ₄ Nb ₆ O ₁₉ •14H ₂ O	Ca ₂ Mn ₂ Nb ₆ O ₁₉ • 20H ₂ O
Space group	R-3	C2/m	P-1
a(Å)	9.0117(6)	15.3444(3)	9.081(4)
b(Å)	9.0117(6)	9.4158(2)	9.982(8)
c(Å)	23.3986(16)	11.2858(4)	10.60(1)
α(°)	90	90	111.07(8)
β(°)	90	118.632(1)	101.15(6)
γ(°)	120	90	99.39(5)
Z	3	2	1
V(Å ³)	1645.64(19)	1431.18(7)	851.5(13)
Strongest PXRD lines d(l)	7.805 (100); 3.250 (33); 2.165 (30)	2.9260 (100); 9.8977 (82); 7.1026 (63)	8.610 (100); 9.282 (36); 3.257 (30)
Optics	Uniaxial (?)	Biaxial (-)	Biaxial(+)

1: Friis *et al.* (2014); 2: Friis *et al.* (2016)